BEST AVAILABLE IMAGES

Defective images within this document are accurate representations of the original documents submitted by the applicant.

Defects in the images may include (but are not limited to):

- BLACK BORDERS
- TEXT CUT OFF AT TOP, BOTTOM OR SIDES
- FADED TEXT
- ILLEGIBLE TEXT
- SKEWED/SLANTED IMAGES
- COLORED PHOTOS
- BLACK OR VERY BLACK AND WHITE DARK PHOTOS
- GRAY SCALE DOCUMENTS

IMAGES ARE BEST AVAILABLE COPY.

As rescanning documents *will not* correct images, please do not report the images to the Image Problem Mailbox.

REMARKS

At the outset, applicants would like to thank Examiner Chernyshev and Primary Examiner Ulm for their time and consideration of the present application at the interview of October 21, 2003. At the interview, the contentions of the outstanding Official Action were discussed.

Applicants believe that the present application has been amended in a manner that places it in condition for allowance at the time of the next Official Action.

Claims 24, 27, 32-33, and 39-43 are pending in the present application. Claims 8-15, 25, 26, 28-31, and 34-38 have been canceled without prejudice and may be the subject of a divisional application. Claims 24, 27, and 32-33 have been amended to more particularly point out and distinctly claim the present invention. New claims 39-43 have been added to vary the scope of the claimed invention. Support for new claims 39-43 may be found in the original claims and in the present specification at page 5, lines 28-30; page 6, lines 1-6; and page 6, lines 6-15.

In the outstanding Official Action, claims 24, 27, and 28 were rejected for reciting the term "non-wildtype". Claims 24 and 27 have been amended to recite "non-wild type". As noted above, claim 28 has been canceled. Support for the term "non-wild type" may be found in the present specification beginning on

page 1. Moreover, applicants note that the original claims also recite this term. Thus, it is believed that claims 24 and 27 have been amended to satisfy the objections of the Official Action.

Claim 26 was rejected under 35 USC 112, first paragraph, as allegedly failing to comply with the written description requirement. It is believed that this rejection has been obviated by the present amendment.

In imposing the rejection, the Official Action alleged that the present specification did not support the recitation to an "active fragment" of an Aβ peptide.

As noted above, claim 26 has been canceled. Moreover, applicants note that none of the claims recite an "active fragment" of Aβ peptide. Thus, applicants believe that claims 24, 27, 32-33 and 39-43 are supported by the present disclosure.

In the outstanding Official Action, claims 24-38 were rejected under 35 USC 112, second paragraph, as allegedly being indefinite. This rejection is respectfully traversed.

The outstanding Official Action rejected the claims for reciting the terms "non-wildtype", "protofibril", and "fibril". As noted above, the claims have been amended to recite a "non-wild type" protofibril. This term is found in the specification and claims and is believed to be understood by one of ordinary skill in the art. Moreover, applicants believe that one of

ordinary skill in the art would also find the terms "protofibril" and "fibril" definite. Indeed, the Examiner's attention is directed to the WALSH et al. article which clearly utilizes this terminology. Thus, it is believed that the claimed invention is definite to one of ordinary skill in the art.

In the Official Action, claims 24-38 were rejected under 35 USC 102(b) as allegedly being anticipated by SCHENK et al. This rejection is respectfully traversed.

Applicants believe that SCHENK et al. fail to disclose or suggest the claimed invention. As noted at the interview, applicants believe that SCHENK et al. fail to disclose or suggest the arctic mutation of the claimed invention.

Indeed, as suggested at the interview by Examiner Chernyshev and Primary Examiner Ulm, amended claim 24 recites a method for the prevention or treatment of Alzheimer's disease in a subject having or suspected of having Alzheimer's disease, comprising administering to the subject a therapeutically effective amount of a non-wild type protofibril, wherein the non-wild type protofibril comprises SEQ ID NO:1. Applicants appreciate the suggestion set forth at the interview and believe that claim 24 is allowable.

The Examiner's attention is also directed to new claims 39-43. Independent claim 39 is directed to a method for the prevention or treatment of Alzheimer's disease. The protofibril

of claim 39 comprises the peptide selected from the group consisting of Aβ39-Arc (Amino Acids 1-39 of SEQ ID NO:1), Aβ40-Arc (Amino Acids 1-40 of SEQ ID NO:1) and Aβ42-Arc (SEQ ID NO:1). As noted above, SCHENK et al. fail to disclose or suggest the arctic mutation. As a result, it is believed that claim 39 is also allowable. Applicants note that claim 40 is dependent on claim 39.

As to independent claim 41, claim 41 recites a method for the prevention or treatment of Alzheimer's disease in a subject having or suspected of having Alzheimer's disease, administering to the subject a therapeutically effective amount of a non-wild type protofibril, wherein the protofibril comprises a mutated Aβ peptide comprising the mutation $Glu_{22} \rightarrow Gly_{22}$. Claim 42 is dependent on claim 41. Applicants believe that claims 41 and 42 are allowable for the reasons noted above. SCHENK et al. do not teach or suggest the arctic mutation.

Claims 27 and 32 are directed to a method for prevention and treatment of Alzheimer's disease, wherein a therapeutically effective antibody is administered to the subject. At this time, applicants would like to clarify the Interview Summary of October 21, 2003. While the Interview Summary recommends limiting the claims to the use of antibodies that bind protofibrils of Arc Aβ to the exclusion of wild type Aβ, applicants note that the present invention is actually

directed to antibodies which have properties that are identical to antibodies raised against Aβ-Arc peptides in a protofibril confirmation. While SCHENK et al. may teach a method of treating Alzheimer's patients with the administration of an antibody to an Aβ peptide, SCHENK et al. fail to disclose or suggest antibodies raised against an Aβ-Arc peptide in a protofibril confirmation. Indeed, SCHENK et al. teach that the antibodies specifically bind at Aβ peptide (see SCHENK et al., page 17, lines 35-39).

Thus, in view of the above, it is believed that SCHENK et al. fail to anticipate or render obvious claims 24, 27, 32, 33, and 39-43.

At this time, applicants would also like to present the article by FORSELL et al. At the interview, Examiner Chernyshev and Primary Examiner Ulm asked that this article be submitted. The article is directed to an amyloid precursor protein mutation at codon 713 (Ala → Val). Thus, the article does not pertain to the arctic mutation of the present invention. Applicants also note that this reference was provided with the Information Disclosure Statement submitted on March 12, 2002 and has already been considered by the Patent Office.

In view of the present amendment and the foregoing remarks, therefore, it is believed that this application is now in condition for allowance, with claims 24, 27, 32-33, and 39-43,

as presented. Allowance and passage to issue on that basis are accordingly respectfully requested.

The Commissioner is hereby authorized in this, concurrent, and future replies, to charge payment or credit any overpayment to Deposit Account No. 25-0120 for any additional fees required under 37 C.F.R. § 1.16 or under 37 C.F.R. § 1.17.

Respectfully submitted,

YOUNG & THOMPSON

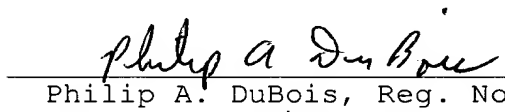

Philip A. DuBois, Reg. No. 50,696
745 South 23rd Street
Arlington, VA 22202
Telephone (703) 521-2297
Telefax (703) 685-0573
(703) 979-4709

PD/fb

APPENDIX:

The Appendix includes the following item(s):

- WALSH et al. "Amyloid β-Protein Fibrillogenesis"

- FORSELL et al. "Amyloid precursor protein mutation at codon 713 (Ala → Val) does not cause schizophrenia: non-pathogenic variant found at codon 705 (silent)"

THE JOURNAL OF BIOLOGICAL CHEMISTRY
© 1997 by The American Society for Biochemistry and Molecular Biology, Inc.

Vol. 272, No. 35, Issue of August 29, pp. 22364–22372, 1997
Printed in U.S.A.

Amyloid β-Protein Fibrillogenesis

DETECTION OF A PROTOFIBRILLAR INTERMEDIATE*

(Received for publication, April 21, 1997, and in revised form, June 18, 1997)

Dominic M. Walsh‡, Aleksey Lomakin‡§, George B. Benedek§, Margaret M. Condron‡, and David B. Teplow‡¶

From the ‡Department of Neurology (Neuroscience), Harvard Medical School, and Biopolymer Laboratory, Brigham & Women's Hospital, Boston, Massachusetts 02115 and the §Department of Physics and Center for Materials Science and Engineering, Massachusetts Institute of Technology, Cambridge, Massachusetts 02139

Fibrillogenesis of the amyloid β-protein (Aβ) is a seminal pathogenetic event in Alzheimer's disease. Inhibiting fibrillogenesis is thus one approach toward disease therapy. Rational design of fibrillogenesis inhibitors requires elucidation of the stages and kinetics of Aβ fibrillogenesis. We report results of studies designed to examine the initial stages of Aβ oligomerization. Size exclusion chromatography, quasielastic light scattering spectroscopy, and electron microscopy were used to characterize fibrillogenesis intermediates. After dissolution in 0.1 M Tris-HCl, pH 7.4, and removal of preexistent seeds, Aβ chromatographed almost exclusively as a single peak. The molecules composing the peak had average hydrodynamic radii of 1.8 ± 0.2 nm, consistent with the predicted size of dimeric Aβ. Over time, an additional peak, with a molecular weight >100,000, appeared. This peak contained predominantly curved fibrils 6–8 nm in diameter and <200 nm in length, which we have termed "protofibrils." The kinetics of protofibril formation and disappearance are consistent with protofibrils being intermediates in the evolution of amyloid fibers. Protofibrils appeared during the polymerization of Aβ-(1–40), Aβ-(1–42), and Aβ-(1–40)-Gln^{22}, peptides associated with both sporadic and inherited forms of Alzheimer's disease, suggesting that protofibril formation may be a general phenomenon in Aβ fibrillogenesis. If so, protofibrils could be attractive targets for fibrillogenesis inhibitors.

Fibrillar amyloid plaques in the cerebral parenchyma and vasculature are a cardinal neuropathologic feature of Alzheimer's disease (AD)[1] (1). Plaques are composed predominantly of insoluble fibers of the amyloid β-protein (Aβ) (2). Aβ is a normal component of the plasma and cerebrospinal fluid, occurring as a soluble 40- or 42-residue peptide (3, 4). Thus, a central question in the etiology of AD is the mechanism(s) by which these soluble Aβ molecules are converted into plaque-associated fibers (5). This question is particularly relevant because Aβ fibers, unlike nonfibrillar Aβ, are neurotoxic *in vitro* and are associated with damaged neuropil *in vivo* (6). These observations suggest that inhibiting fiber formation would be an effective approach toward AD therapy. However, if these efforts are to succeed, fiber formation must be understood at the molecular level.

Aβ fibrillogenesis is a nucleation-dependent polymerization process (7, 8). The kinetics of this type of process is controlled by two key parameters, nucleation rate and elongation rate. Past studies of the kinetics of Aβ fibrillogenesis, utilizing techniques including turbidity, sedimentation, and thioflavine T binding, could only provide information on the appearance of high molecular weight aggregates (7, 9) or the disappearance of soluble peptide (10–13). Neither rate constants nor structures of fibrillogenesis intermediates could be determined by these approaches. In contrast, the technique of quasielastic light scattering spectroscopy (QLS) is particularly well suited for resolving individual stages of polymerization processes and for examining polymerization kinetics (14). QLS was used initially to monitor late stages of Aβ fibrillogenesis (15, 16). Recently, however, a model system was developed for the highly reproducible growth of Aβ fibers (8). This allowed QLS monitoring of polymer size during all phases of fibrillogenesis and determination of the rates of Aβ fibril nucleation and elongation (8).

The QLS approach is less useful for studying small structures, such as Aβ monomers and oligomers, when they exist in mixtures with larger polymers. Because these prefibrillar intermediates are potential targets for fibrillogenesis inhibitors, it is important to characterize them. One method for doing so is SDS-PAGE (17–20). However, since many Aβ polymers are SDS-labile, interpreting SDS-PAGE studies of Aβ polymerization is problematic. Size exclusion chromatography (SEC) is an attractive alternative to SDS-PAGE because it fractionates on the basis of molecular weight and is performed using nondenaturing and nondisaggregating buffers. SEC has been used to study the aggregation state of Aβ in solution (20–23), but its potential in kinetic studies has not been exploited. We report here the use of SEC, coupled with QLS and electron microscopy, to characterize the temporal evolution and structures of oligomeric intermediates in the pathway of Aβ fibrillogenesis.

EXPERIMENTAL PROCEDURES

Chemicals and Solvents

Chemicals were obtained from Sigma and, unless otherwise stated, were of the highest purity available. Solvents were HPLC grade and were obtained from Fisher. Water was double-distilled and deionized using a Milli-Q system (Millipore Corp., Bedford, MA).

* This work was supported in part by National Institutes of Health Grants 1P01AG14366 (to D. B. T.) and 5R37EY05127 (to G. B. B.) and by the Foundation for Neurologic Diseases (to D. B. T.). The costs of publication of this article were defrayed in part by the payment of page charges. This article must therefore be hereby marked "*advertisement*" in accordance with 18 U.S.C. Section 1734 solely to indicate this fact.

¶ To whom correspondence should be addressed: Brigham & Women's Hospital, 77 Avenue Louis Pasteur (HIM-756), Boston, MA 02115. Tel.: 617-525-5270; Fax: 617-525-5252; E-mail: teplow@end.bwh.harvard.edu.

[1] The abbreviations used are: AD, Alzheimer's disease; Aβ, amyloid β-protein; QLS, quasielastic light scattering spectroscopy; PAGE, polyacrylamide gel electrophoresis; SEC, size exclusion chromatography; HPLC, high pressure liquid chromatography; HFIP, 1,1,1,3,3,3-hexafluoro-2-propanol; RIA, radioimmunoassay; Tricine, *N*-[2-hydroxy-1,1-bis(hydroxymethyl)ethyl]glycine.

Peptides

Peptides were synthesized as described by Lomakin *et al.* (8). Crude Aβ-(1–40) was purified by reverse phase HPLC using a Vydac phenyl column (22 × 250 mm) and a linear gradient of 28–56% B over 50 min (A: 0.1% (v/v) trifluoroacetic acid; B: 70% (v/v) acetonitrile (CH_3CN), 0.09% (v/v) trifluoroacetic acid) at a flow rate of 20 ml/min. Aβ-(1–42) was purified using a PLRP-S column (25 × 150 mm) and a linear gradient of 20–60% B over 80 min (A: 50 mM Tris-HCl, pH 9.1; B: 50 mM Tris-HCl, pH 9.1, containing 54% (v/v) CH_3CN and 6% (v/v) 2-propanol) at a flow rate of 15 ml/min (24). Following purification, Aβ-(1–42) was dialyzed against 0.15 M ammonium hydroxide in 40% (v/v) CH_3CN, lyophilized, and converted to its trifluoroacetic acid salt by dissolution in 100% trifluoroacetic acid. Peptide mass, purity, and quantity were determined by a combination of matrix-assisted laser desorption/ionization time-of-flight mass spectrometry, analytical HPLC, and quantitative amino acid analysis, respectively. Purified peptides were aliquoted, lyophilized, and stored at −20 °C until used. Aβ-(40–1) was generously provided by Dr. Dennis Selkoe (Brigham & Women's Hospital and Harvard Medical School).

SEC

Columns and Buffers—A description of columns and buffers is found in Table I. Superdex, Superose and TSK columns were attached to a Rainin HPLC system consisting of a HPXL pump, a Rheodyne 7161 injector, and a Dynamax UV-1 detector. Columns were eluted at a flow rate of 0.5 ml/min and peptides detected by UV absorbance at 254 nm. Sephadex G-50 (superfine) media were prepared using either 1 × 30 cm or 1 × 50 cm borosilicate Econo-columns (Bio-Rad, Hercules, CA) and eluted at 0.17 ml/min using an LKB Microperpex S peristaltic pump. Peptides were detected by UV absorbance at 254 nm using a Pharmacia UV-1 single path monitor. Each experiment was performed at least two times. Pre-packed columns were washed with 50% (v/v) formic acid between experiments. Sephadex columns were prepared from fresh resin prior to each experiment.

Sample Preparation—400 μg of Aβ-(1–40) were dissolved in 200 μl of water and then vortexed briefly. 200 μl of 2 × buffer were then added, and the sample was vortexed again. Following centrifugation (17,000 × *g*, 3 min), 100 μl of the supernatant was chromatographed. For kinetic analyses, samples were incubated at room temperature for various periods prior to centrifugation. For quasielastic light scattering spectroscopy, electron microscopy, and gel electrophoresis, Aβ-(1–40) was dissolved at a concentration of 2 mg/ml (0.46 mM), incubated at room temperature for 48 h, and then chromatographed as above. Similarly, Aβ-(1–40)-Gln^{22} and Aβ-(1–42) were dissolved at concentrations of 1 mg/ml (0.23 and 0.22 mM, respectively) and incubated at room temperature for 6 h, and then 300 μl of each were chromatographed as above. Peak fractions of 50–200-μl volume were collected and analyzed.

Preparation of "Seedless" Samples—Disaggregation experiments were performed by dissolving 800 μg of Aβ-(1–40) in 160 μl of 1,1,1,3,3,3-hexafluoro-2-propanol (HFIP) and incubating at room temperature for 10 min. The HFIP was removed by evaporation under a gentle stream of argon, leaving a slightly yellow film that was resuspended in 80 μl of dimethyl sulfoxide (Me_2SO) and sonicated for 30 min. The solution was then filtered through an Anotop 10 Plus filter (20 nm, Whatman Inc., Clifton, NJ) and diluted 1:9 (v/v) with 0.1 M Tris-HCl, pH 7.4, containing 0.02% (w/v) sodium azide (Tris buffer). After centrifugation (17,000 × *g*, 3 min), 100 μl of supernatant were injected onto a Superdex 75 column. The remainder of the solution was incubated at room temperature and sampled at 1, 4, 8, and 24 h.

Radiotracer Experiments—To search for low abundance intermediates, radioiodinated Aβ-(1–40) (^{125}I-Aβ, ~2000 Ci/mmol) was prepared according to Maggio *et al.* (25) at a final concentration of 100 pM in Tris buffer containing 0.5% (v/v) Me_2SO. After incubation at room temperature for 0, 8, or 24 h, samples were centrifuged (17,000 × *g*, 3 min), and 100-μl aliquots were injected onto a Superdex 75 column. 0.5-ml fractions were collected, and their radioactivity was determined by scintillation counting. To examine the effect of varying Aβ concentration, 3 μl of appropriately diluted Aβ-(1–40) were added to 597 μl of Tris buffer containing 100 pM ^{125}I-Aβ, to yield final Aβ concentrations of 1×10^{-10}, 1×10^{-9}, 1×10^{-7}, 1×10^{-6}, and 2.3×10^{-4} M. Samples were then incubated and analyzed as above.

Radioimmunoassay (RIA) of Column Fractions—A RIA procedure was used to detect trace levels of oligomeric fibril intermediates. Aβ-(1–40) was dissolved in HFIP, lyophilized, dissolved to a suitable concentration in Me_2SO, and then diluted 1:200 (v/v) with 0.1 M Tris buffer. Final Aβ concentrations were 1×10^{-7}, 1×10^{-8}, 1×10^{-9}, and 1×10^{-4} M. Samples were then incubated and chromatographed as in the radiotracer experiments. Fractions were frozen at −20 °C until assayed. Aβ-(1–40) content in each fraction was determined by RIA (26).

QLS

Fractions from SEC were collected directly into cuvettes and analyzed within 1 min of elution. QLS was carried out essentially as described (8). Measurements were performed at 25 °C using a Langley Ford model 1097 autocorrelator and Coherent argon ion lasers (model Innova 90 or Innova 90-plus) operated at 514 nm.

Electron Microscopy

10 μl of sample were applied to carbon-coated Formvar grids (Electron Microscopy Sciences, Washington, PA) and incubated for 60 s. The droplet was then displaced with an equal volume of 0.5% (v/v) glutaraldehyde solution and incubated for an additional 60 s. The grid then was washed with four or five drops of water and wicked dry. Finally, the peptide was stained with 10 μl of 2% (w/v) uranyl acetate solution (Ted Pella, Inc., Redding, CA) for 2 min. This solution was wicked off, and the grid was air-dried. Samples were examined using a JEOL CX100 electron microscope. To examine insoluble material, pellets of Aβ were suspended in a small volume of buffer and prepared as above.

Gel Electrophoresis

SDS-PAGE was carried out on 16.5% Tricine gels as described by Schagger and Von Jagow (27). Aliquots of each chromatographic fraction (20 μl) were mixed with 3 × SDS sample buffer (10 μl) and boiled for 5 min immediately prior to electrophoresis. Gels were silver-stained using the Bio-Rad silver stain kit and photographed.

RESULTS

Oligomerization of Aβ-(1–40)—To monitor oligomerization of Aβ, an analytical method is necessary that can resolve monomeric Aβ and its oligomers under nondenaturing, nondisaggregating conditions. We reasoned that SEC would be appropriate for this purpose. Initial analysis of presumably monomeric Aβ revealed a single peak with a molecular weight of 10,000 (Table I). This unexpectedly high molecular weight suggested that Aβ might not be monomeric or was partially excluded from the column matrix, indicating a nonideal analyte-matrix interaction.

Because accurate molecular weight determination was critical for the proper interpretation of our experiments, we determined whether the chromatographic behavior of Aβ varied depending on column matrix or elution conditions (Table I). When Aβ-(1–40) from the same peptide lot was dissolved in phosphate-buffered saline and chromatographed on Superdex 75 (dextran-agarose), Superose 12 (agarose), or TSK (silica) matrices, the relative molecular weight of Aβ varied from 10,000 to 18,000. Similarly, when Aβ-(1–40) was dissolved in 0.1 M Tris-HCl, pH 7.4, and then analyzed, molecular weights of 9,000–15,000 were observed. Other solvent conditions resulted in M_r values ranging from 5,000 to 10,500. One explanation for the variations in M_r was nonideal chromatographic behavior of Aβ. This was confirmed in experiments in which the elution buffer was modified by the addition of ethylene glycol, an agent used to inhibit solute-column interactions. Under these conditions, a concentration-dependent decrease in Aβ M_r from 10,000 to 6,000 was seen. We also found that M_r values varied depending on the calibration standards used. Thus, for consistency, all columns were calibrated using the same five standards.

In each experiment, Aβ-(1–40) chromatographed as a single peak in the included volume of the column, but because of its nonideal behavior, the oligomerization state of Aβ within these peaks was unclear. If noncovalent multimers composed these peaks, then treating Aβ with strong denaturants or solvents prior to chromatography might disaggregate these complexes and reduce the M_r. In fact, pretreatment of Aβ with SDS-PAGE sample buffer, Me_2SO, HFIP, or 90% formic acid, had no effect on its M_r. In addition, Aβ-(40–1), the "reverse" peptide of Aβ-(1–40) and one that does not polymerize readily, co-eluted with

TABLE I
Chromatographic properties of Aβ-(1–40)

Aβ-(1–40) was chromatographed on five different size exclusion media, as described under "Experimental Procedures." For each study, the appropriate column was equilibrated with at least three column volumes of elution buffer and then calibrated with five molecular weight standards: avian ovalbumin (44,000); equine myoglobin (17,000); equine cytochrome C (12,384); bovine aprotinin (6,500); and vitamin B_{12} (1,950). Standard curves were constructed by regression analysis and used to determine the molecular weights of analytes. Each condition yielded one peak, which decreased in size over 24 h. A small void peak appeared after 24 h of incubation in some experiments.

Column	Separation range (kDa)	Elution buffer[a]	Aβ M_r	Void peak	Correlation coefficient (r^2)
Superdex 75 (1 × 30 cm)	3–70	PBS	10,000	–	0.98
		PBS, 20% sucrose	10,500	–	0.98
		PBS, 20% MPD	9,000	–	0.96
		PBS, 20% ethylene glycol	8,000	±	0.98
		PBS, 50% ethylene glycol	6,000	±	0.98
		0.1 M Tris-HCl, pH 7.4	15,000	+	0.81
Superdex 200 (1 × 30 cm)	10–600	0.1 M Tris-HCl, pH 7.4	14,000	+	0.77
Superose 12 (1 × 30 cm)	1–300	0.1 M Tris-HCl, pH 7.4	15,000	+	0.79
		PBS	12,000	±	0.92
TSK G2000sw (0.7 × 30 cm)	5–100	0.1% trifluoroacetic acid	8,000	–	0.85
		PBS	18,000	±	0.58
G50sf (1 × 28 cm)	1.5–30	0.1 M Tris-HCl, pH 7.4	9,000	–	0.98
G50sf (1 × 28 cm)		TBS	8,000	–	1.0
G50sf (1 × 47 cm)		TBSE	7,500	–	0.98
G50sf (1 × 47 cm)		50 mM ammonium acetate, pH 7.4	5,000	–	0.98

[a] MPD, 2-methyl-2,4-pentanediol; PBS, phosphate-buffered saline; TBS, Tris-buffered saline; TBSE, 0.02 M Tris-HCl, pH 7.4, containing 0.1 M NaCl and 50 μM EDTA.

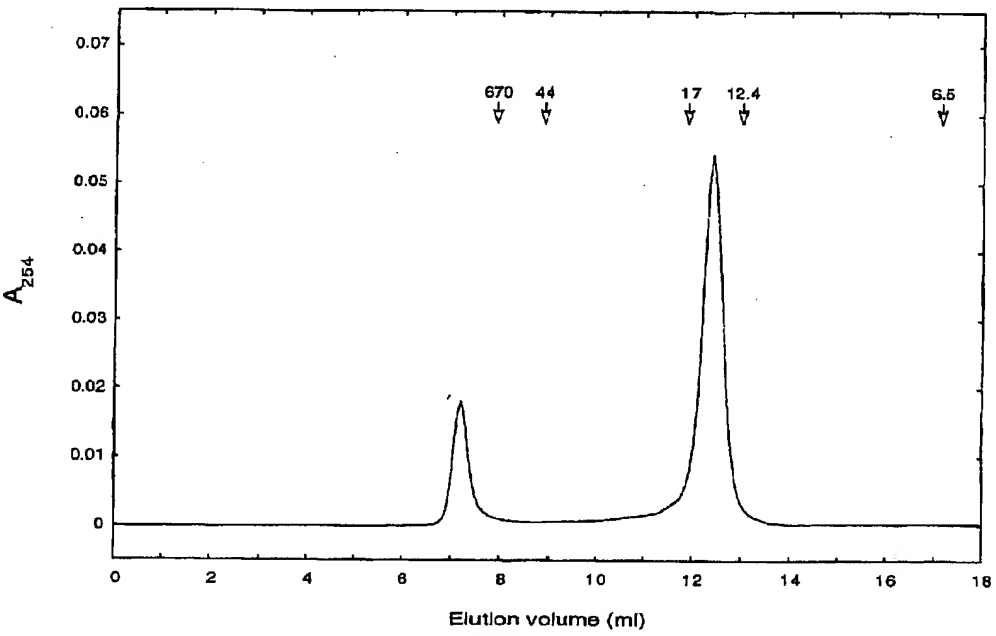

FIG. 1. **Size exclusion chromatography of Aβ.** Aβ-(1–40) was dissolved in 0.1 M Tris buffer at a concentration of 2 mg/ml and chromatographed on a Superdex 75 column, as described under "Experimental Procedures." The gel-included peak elutes at ~12.4 ml, while the gel-excluded peak elutes at ~7.2 ml. Elution positions of molecular weight standards are indicated by *arrows*. Molecular masses are indicated in kDa.

Aβ-(1–40) on the Superdex 75/Tris-HCl system (data not shown).

A time-dependent decrease in the magnitude of the gel-included peak was observed under all conditions examined (data not shown). In the Superdex 75/Tris-HCl system, this decrease was accompanied by the appearance of a new peak in the void volume of the column (Fig. 1). For linear polymers such as dextran, this would be consistent with a molecular weight in excess of 30,000. To better estimate the size of the aggregates in this peak, chromatography was also performed on Superdex 200 and Superose 12 columns, which have exclusion limits (for dextrans) of ~100 kDa. A peak was observed in the void volume

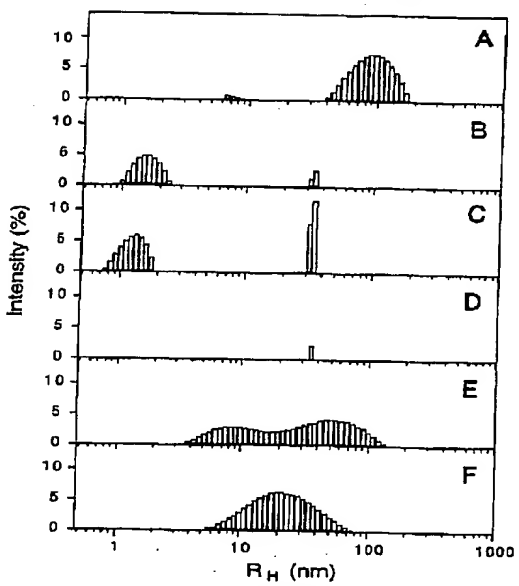

FIG. 2. **Analysis of Aβ size by QLS.** Samples included soluble Aβ-(1–40) obtained by dissolution in 0.1 M Tris-HCl and centrifugation for 3 min at 17,000 × *g* (*A*); the gel-included fraction obtained following SEC of the supernatant from A (*B*); aprotinin (6,500 Da) (*C*); buffer alone (*D*); soluble Aβ-(1–40) following dissolution in 0.1 M Tris-HCl, incubation at room temperature for 48 h, and centrifugation for 3 min at 17,000 × *g* (*E*); and the gel-excluded fraction obtained by SEC of Aβ-(1–40) (*F*) prepared as in *E*. Each R_H distribution was normalized to 100% intensity. In *A*, *E*, and *F*, scattering intensity comes predominately from polymeric and aggregated Aβ. In *B*, *C*, and *D*, scattering from the buffer (R_H < 0.2 nm; data not shown) accounts for the remaining scattering, and signals at 35 nm are not peptide-related, since they are present in buffer alone. Comparison of the magnitudes of intensities among experiments is not meaningful.

of these columns as well, suggesting that the Aβ multimers had molecular masses in excess of 100 kDa, or that they too behaved anomalously on SEC. Experiments using Aβ-(1–42) yielded essentially identical results (data not shown).

Size Determination of Aβ—To estimate the actual sizes of Aβ particles in the peaks obtained by SEC, QLS was used to measure the average diffusion coefficient of the particles. Particle size is expressed as the radius of a sphere with an identical diffusion coefficient. This quantity is termed the hydrodynamic radius (R_H) (for a review, see Ref. 28) and is conceptually equivalent to a Stoke's radius in gel permeation chromatography. For spherical particles, $R_H = r$, where r is the geometric radius. For a fibril, R_H depends on the length, diameter, and flexibility of the particle. R_H is always less than the radius of the sphere circumscribed around the particle.

Immediately after dissolution in Tris-HCl and centrifugation (17,000 × *g*, 3 min), but prior to SEC, soluble Aβ-(1–40) had an average R_H of ~40–200 nm (Fig. 2*A*). Because scattering intensity is proportional to molecular weight, monomers and small oligomers can be difficult to detect in the presence of larger polymers and aggregates. However, by fractionating the Aβ mixture using SEC, we observed a gel-included fraction, with an extrapolated molecular weight of 15,000, which had an average R_H of 1.8 ± 0.2 nm (Fig. 2*B*). Geometric considerations predict that a 4,331-Da peptide in dimeric form will have a R_H = 1.6–2.1 nm. For comparison, QLS analysis of aprotinin (6,500 Da) fractionated by SEC yielded an average R_H of 1.6 ± 0.6 nm (Fig. 2*C*). These data argue that Aβ existed as a dimer[2] in the gel-included fraction, not as a trimer or tetramer as suggested by SEC.

We next sought to determine the size(s) of the Aβ oligomers in the gel-excluded fraction. To produce sufficient material for analysis, Aβ-(1–40) was incubated for 48 h prior to chromatography. QLS analysis of the pre-SEC supernatant (17,000 × *g*) revealed a broad distribution of particles sizes (range 4 to >100 nm) (Fig. 2*E*). Comparison of this distribution with that obtained from Aβ immediately after dissolution (Fig. 2*A*) shows that particles of intermediate size form during fibrillogenesis. Dimers were not resolved clearly in this experiment due to the predominance of larger Aβ oligomers/polymers, as discussed above. QLS analysis of the gel-excluded peak showed that the majority of intermediate particles ranged in size from ~10 to 50 nm (Fig. 2*F*). For a solution of noninteracting rods with diameters of 8 nm, this range corresponds to lengths of 80–500 nm. These lengths would be significantly smaller if rod-rod interactions were occurring. On the other hand, if the rods were flexible, the lengths would be even larger.

Taken together, our SEC and QLS data indicate that the gel-included peak contained dimeric Aβ, the gel-excluded peak contained a distribution of oligomers, and the pellet obtained prior to chromatography was composed of higher molecular weight polymers and aggregates.

Morphology of Aβ Oligomers—To determine the morphology of the Aβ species observed in the SEC experiments, electron microscopy was performed. For both Aβ-(1–40) and Aβ-(1–42), no structures were detected in the gel-included fractions, while the 17,000 × *g* pellets obtained prior to chromatography contained a mesh of fibers 6–10 nm in diameter (Fig. 3, *A* and *B*). These fibers were indistinguishable from those found in senile plaques (29). In addition, particularly in the case of Aβ-(1–42), short fibrils were seen associated with the longer fibers. Generally, one end of each fibril appeared to adhere to the side of a fiber, while the other end was free. Similar fibrils were found in the void volume peaks, where they appeared as short, curly fibrils 6–10 nm in diameter and 5–160 nm in length, on average (Fig. 3, *C* and *D*). We have termed these structures "protofibrils" to distinguish them from the mature, amyloid-type fibers found in the pellets.

Chromatographic Analysis of Seedless Aβ—Low molecular weight oligomers (larger than dimers) were not detected in the prior SEC experiments. Oligomerization could be thermodynamically unfavorable or be suppressed kinetically due to rapid consumption of precursor by growing fibrils. Fibril formation would be accelerated by the presence of pre-existing aggregates (seeds) in the starting material. Freshly prepared solutions of Aβ-(1–40) did, in fact, contain high molecular weight species that might act as seeds (Fig. 2*A*). To determine if rapid fibril formation affected Aβ oligomerization, we sought to eliminate seeds prior to our experiments by dissolving Aβ in HFIP, lyophilizing the solution, dissolving the lyophilizate in Me_2SO, and then filtering the solution through a filter containing 20-nm pores. The chromatographic behavior of peptides "deseeded" in this way did not differ from that of peptides prepared without deseeding (data not shown). An included peak was observed initially, which was replaced over time by a peak in the void volume of the column. These data suggest that formation of stable low molecular weight oligomers is a relatively unfavored process.

High Sensitivity Monitoring of Aβ Polymerization—Our re-

[2] For simplicity, Aβ within the gel-included peak will be referred to as "dimeric." However, the QLS data alone do not eliminate the possibility that Aβ within this peak is monomeric.

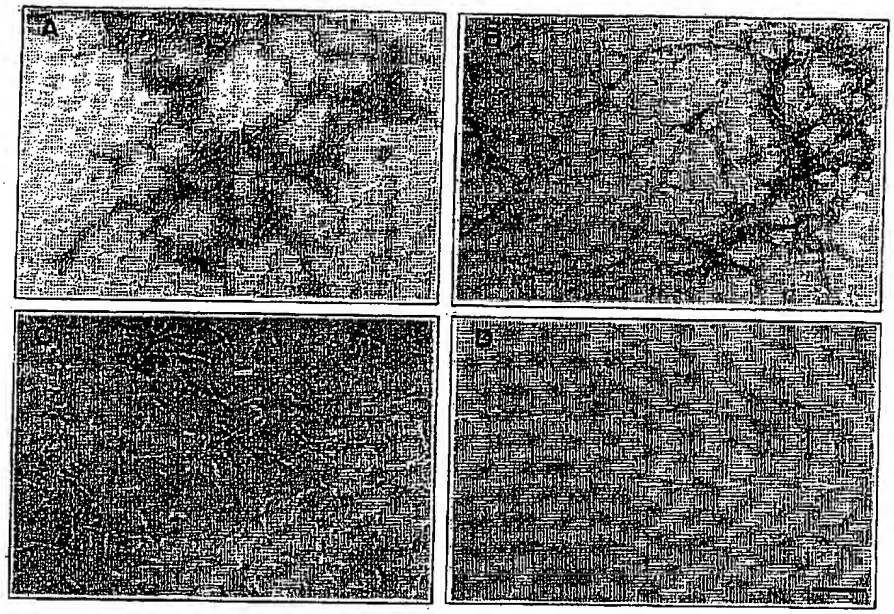

FIG. 3. **Morphology of Aβ polymers fractionated by size exclusion chromatography.** Electron microscopy was performed on prechromatography pellets of Aβ-(1–40) (*A*) and Aβ-(1–42) (*B*) and on the void peaks of Aβ-(1–40) (*C*) and Aβ-(1–42) (*D*). *Scale bar*, 100 nm.

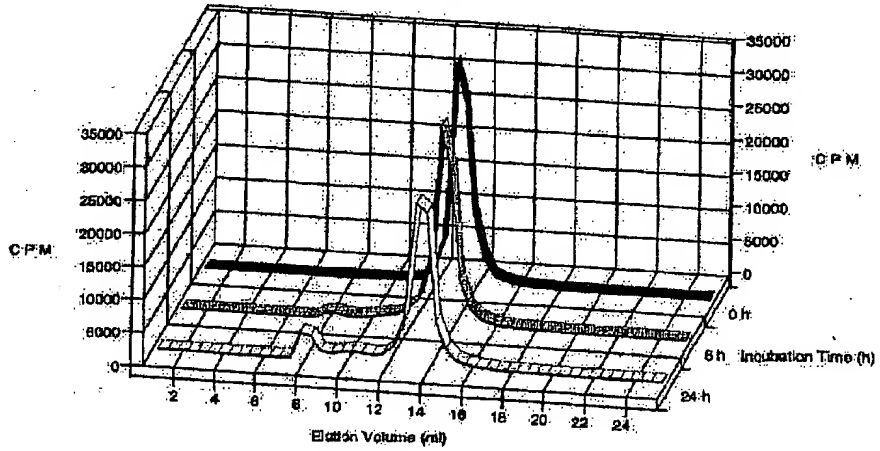

FIG. 4. **High sensitivity size exclusion chromatography of Aβ-(1–40).** ^{125}I-Aβ-(1–40) was added to a freshly prepared solution of Aβ-(1–40) (1 mg/ml) and fractionated on a Superdex 75 column after 0, 8, and 24 h of incubation. The ^{125}I-Aβ-(1–40) content of the fractions was determined by scintillation counting. The chromatograms shown are representative of results from three independent experiments.

sults suggested that, if present, steady state levels of oligomeric fibril precursors would be extremely low, making their detection by UV absorbance difficult. For this reason, two sensitive methods were utilized to monitor Aβ polymerization: 1) radioiodinated peptide was used as a tracer in mixtures with unlabeled peptide; and 2) SEC fractions were assayed for Aβ content by RIA. Radioiodinated Aβ-(1–40) (^{125}I-Aβ-(1–40); 100 pM final concentration) was mixed with unlabeled Aβ (1 mg/ml) in 0.1 M Tris-HCl, pH 7.4, chromatographed on a Superdex 75 column, and detected in column fractions by scintillation counting. At 0 h, a single peak was observed coincident with unlabeled Aβ (Fig. 4). After incubation at room temperature for 8 or 24 h, an additional peak of radioactivity was detected in the void volume (Fig. 4; at ~7.4 ml). The radioactivity and UV absorbance of this peak increased at the same rate over time, suggesting that the labeled and unlabeled peptides polymerized in an analogous manner.

In the above experiment, given that ~33,000 cpm of Aβ were

used, oligomers representing as little as 1% of the initial protein mass could have been detected. Asymmetry in the void and dimer peaks, indicated by trailing and leading shoulders, respectively, mirrored the behavior of the unlabeled peptide (*cf.* Figs. 1 and 4). RIA analysis of Aβ-(1–40) SEC fractions produced using the same protocol as above yielded results similar to those presented in Fig. 4 (data not shown). Experiments were also performed at much lower Aβ concentrations by using tracer alone; however, below 10^{-5} M, recovery of ^{125}I-Aβ-(1–40) from the column was poor, probably due to nonspecific adsorption to the column matrix and associated glass and plastic surfaces (22, 30). Taken together, these data suggest that although oligomeric intermediates do exist, they do not accumulate to a significant degree during the polymerization process.

Kinetics of Protofibril Formation—As a first step to determining the key primary structural elements of Aβ that control the kinetics of dimer and protofibril utilization, comparative polymerization studies were done using Aβ-(1–42), Aβ-(1–40), and Aβ-(1–40) containing the substitutions Phe^{19} → Pro (31), Ala^{21} → Gly (32), or Glu^{22} → Gln (33). Peptides were dissolved in Tris-HCl, pH 7.4, at concentrations of 1 mg/ml, incubated for up to 24 h, and then their polymerization states were analyzed by SEC on a Superdex 75 column.

Immediately after dissolution, all samples produced a single chromatographic peak with a retention time equivalent to that of dimeric wild type Aβ-(1–40). The level of the Aβ-(1–40) peak declined by ~20% over 24 h, while the levels of the Aβ-(1–40)-Pro^{19} and Aβ-(1–40)-Gly^{21} peaks declined <10% (Fig. 5*A*). Aβ-(1–42) and Aβ-(1–40)-Gln^{22} peaks decreased rapidly initially, with a ~40% decrease within 1 h, followed by a slower decrease down to 20–30% of initial levels by 24 h (Fig. 5*A*). The inverse was observed for the protofibril peaks (Fig. 5*B*). The levels of protofibrils produced by Aβ-(1–40) and Aβ-(1–40)-Gly^{21} increased ~15 and ~5%, respectivuly, over the first 24 h. No protofibril peak was detected at 24 h in experiments with Aβ-(1–40)-Pro^{19}. In contrast, the levels of protofibrils formed by Aβ-(1–42) and Aβ-(1–40)-Gln^{22} increased rapidly within the first hour. Peak levels of protofibrils were seen after 8 h for Aβ-(1–42) and after 1 h for Aβ-(1–40)-Gln^{22}, after which these levels declined. The continuous decline in levels of the included peak, coupled with the transitory appearance of protofibrils, is consistent with the protofibril being an intermediate in Aβ fibrillogenesis.

SDS-PAGE of Aβ Oligomers—SDS-stable oligomers have been detected previously in media from cultured cells secreting Aβ (34). To determine the SDS stability of the oligomers observed during SEC, peak fractions were analyzed by SDS-PAGE. Interestingly, dimer, protofibril (void), and fiber (pellet) fractions produced during polymerization of Aβ-(1–40) all produced a single 4-kDa band (Fig. 6*A*). To identify trace levels of oligomers, ^{125}I-Aβ-(1–40) was incubated with Aβ-(1–40), and the resulting products were characterized autoradiographically following gel electrophoresis. A single 4-kDa band was observed in this experiment as well (data not shown). Electrophoresis of SEC fractions of Aβ-(1–42) produced a different pattern (Fig. 6*B*). Void peak fractions produced five bands, corresponding in mass to monomeric through pentameric Aβ (Fig. 6*B*, *lanes 2–4*). The dimer peak of Aβ-(1–42) ran as a single 4.5-kDa band (Fig. 6*B*, *lanes 5* and *6*). Prechromatography pellets (see "Experimental Procedures"), which contained fully formed Aβ fibers, produced the same five bands as did the void peak fractions, plus an occasional gel-excluded band (Fig. 6*B*, *lane 1*). These data show that SDS disaggregates Aβ fibers and protofibrils down to monomers, in the case of Aβ-(1–40), or to monomers and low molecular weight oligomers, in the case of Aβ-(1–42).

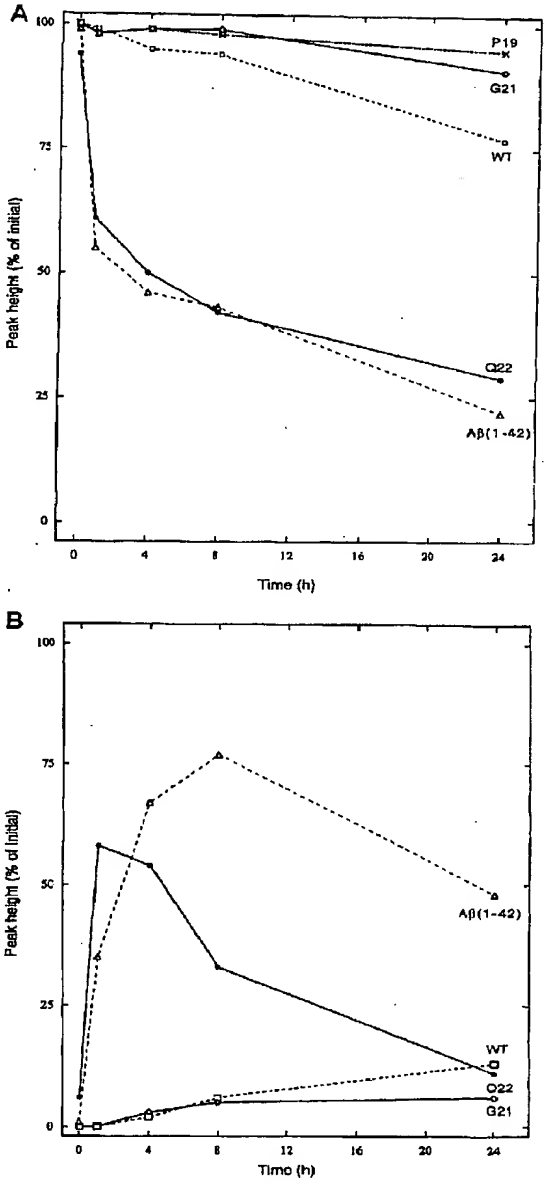

FIG. 5. **Kinetics of Aβ polymerization.** Aβ peptides were allowed to polymerize for 0, 1, 4, 8, and 24 h and then were fractionated by SEC (see "Experimental Procedures"). Amounts of dimeric Aβ (*A*) and protofibrils (*B*) are plotted as a percentage of the levels at time 0, which were assigned a value of 100%. Experiments were done in duplicate. *WT*, wild type; *P19*, Phe^{19} → Pro; *G21*, Ala^{21} → Gly; *Q22*, Glu^{22} → Gln.

DISCUSSION

Accumulating evidence supports the hypothesis that Aβ fibrillogenesis is a seminal pathogenetic event in AD (35, 36).

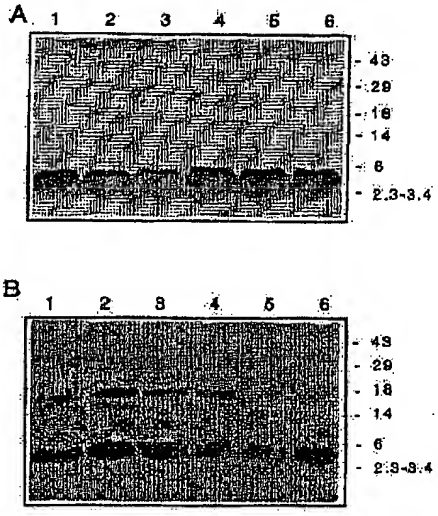

FIG. 6. **SDS-PAGE analysis of SEC fractions.** Aβ-(1–40) (*A*) and Aβ-(1–42) (*B*) were dissolved in 0.1 M Tris-HCl, pH 7.4, incubated 6–48 h, and then analyzed by SEC, as described under "Experimental Procedures." The prechromatography pellets (*lanes 1*), void peak fractions (*lanes 2–4*), and fractions from the dimer peaks (*lanes 5–6*) were then analyzed by SDS-PAGE and silver staining.

Inhibiting or reversing fibrillogenesis is thus a logical therapeutic strategy. The goal of the experiments reported here was to characterize, structurally and kinetically, the initial stages of Aβ fibrillogenesis to identify targets for fibrillogenesis inhibitors. We have discovered a potential target, the amyloid protofibril, which appears to be an important intermediate in Aβ fibrillogenesis. This discovery, and the unique constellation of methods used to achieve it, have implications both for our understanding of Aβ fibrillogenesis and for the methodological approaches used to study Aβ polymerization.

In our SEC studies of Aβ-(1–40) polymerization, a single peak was observed following dissolution of lyophilized peptide (Table I). The M_r of this peak varied from 5 to 18 kDa, depending on the solvents and columns used, corresponding to monomeric to tetrameric Aβ. These molecular weight estimations and, in fact, those of other groups using SEC (20–23, 37, 38) were based on calibration curves derived using soluble peptides and proteins specially selected for their ideal chromatographic behavior. However, we found that Aβ, under nondenaturing conditions, did not chromatograph ideally. This behavior is not uncommon for amphipathic peptides, such as Aβ, which may undergo both electrostatic and/or hydrophobic interactions with the column matrix (39). For example, nonideal chromatographic behavior has recently been reported for both the nonamyloid component of AD amyloid (40) and melittin (41). Therefore, to be able to estimate accurately the molecular weights, and thus the oligomerization states, of Aβ using SEC, new standardization methods had to be utilized.

QLS is a particularly powerful and appropriate technique for monitoring the sizes of protein polymers in solution (for a review, see Ref. 28). By coupling SEC with QLS, the oligomerization state of Aβ within different chromatographic fractions could be estimated directly, rapidly, and noninvasively. We found that Aβ-(1–40) and Aβ-(1–42) exhibit predominantly three forms in aqueous solution: dimer, protofibril, and fiber. Metastable oligomers (dimer < M_r < protofibril) were detected using highly sensitive radiochemical and immunological assays; however, none accumulated in significant quantities. Aβ-(1–40) and Aβ-(1–42) have been reported to form stable dimers (20, 23) as well as high molecular weight polymers (20), although these latter structures were not characterized. Our analysis of protofibril fractions by QLS revealed a R_H distribution of 10–50 nm. Assuming Aβ forms rods with an 8-nm average diameter, and recognizing that in polydisperse populations of polymers the larger particles skew the R_H distribution toward higher values, the QLS data were consistent with protofibrils 30–500 nm in length. These estimates were consistent with results of electron microscopy, which revealed curly fibrils 6–10 nm in diameter and ranging in length up to 200 nm.

An important question arising from the discovery of the protofibril was where it lay in the pathway of Aβ fibrillogenesis. In an effort to answer this question, SEC was used to study the stages and kinetics of Aβ fibrillogenesis. In the cases of Aβ-(1–42) and Aβ-(1–40)-Gln^{22}, dimers predominated initially, and then a time-dependent decrease in dimer levels was paralleled by an increase in protofibrils. Finally, protofibril levels declined as well. Radiochemical analyses of SEC fractions showed that only two discrete Aβ species, dimer and protofibril, accumulated during fibrillogenesis. However, trailing and leading shoulders associated with protofibril and dimer peaks, respectively, appeared during fibrillogenesis. In addition, an elevated base line was observed between the protofibril and dimer peaks. These data are consistent with a polymerization process in which Aβ oligomerizes through a series of short lived intermediates to form protofibrils, which act as centers for the growth of mature fibers. A similar pathway has been proposed by Harper *et al.* (42) based on studies of Aβ polymerization monitored by atomic force microscopy.

Rates of dimer utilization and protofibril formation varied markedly among different Aβ species (Fig. 5). The differences observed agree qualitatively with previous reports indicating that structural elements in the central hydrophobic core (Leu^{17}–Ala^{21}) and at the COOH terminus of Aβ play key roles in controlling fibrillogenesis (7, 11, 43–46). For example, relative to wild type Aβ-(1–40), both Aβ-(1–40)-Gln^{22} and Aβ-(1–42) polymerize into protofibrils and then into fibers significantly faster. In each case, amino acid substitutions (Glu^{22} → Gln^{22}) or additions (Ile^{41}-Ala^{42}) produce peptides of greater hydrophobicity, a change that could drive aggregation through the hydrophobic effect (47). Whether significant intramolecular or intermolecular structural changes also contribute to the altered kinetics is unknown. In contrast, Aβ-(1–40)-Gly^{21} polymerized more slowly than did wild type peptide, while Aβ-(1–40)-Pro^{19} remained almost completely unpolymerized. Few protofibrils were formed by Aβ-(1–40)-Gly^{21} after 24 h, and none were observed in the Aβ-(1–40)-Pro^{19} samples. These results suggest that glycine and proline alter Aβ structure in a manner that inhibits or precludes the self-associations necessary to produce protofibrils and fibers. This could occur through destabilization of structural elements, including α-helices and/or β-strands (48, 49), required for fiber formation. This mechanism has been implicated in alterations in βPP processing induced by familial AD mutations (31, 50) and is consistent with previous findings that fibril formation requires formation of a stable β-sheet structure (11, 44, 51, 52).

In addition to SEC, denaturing gel electrophoresis (SDS-PAGE) has been used to characterize Aβ oligomers (17–20). However, on theoretical grounds (*i.e.* the use of the chaotrope SDS), this technique would be expected to disaggregate noncovalent complexes, limiting its usefulness in studies of protein aggregation. We examined this issue by comparing results

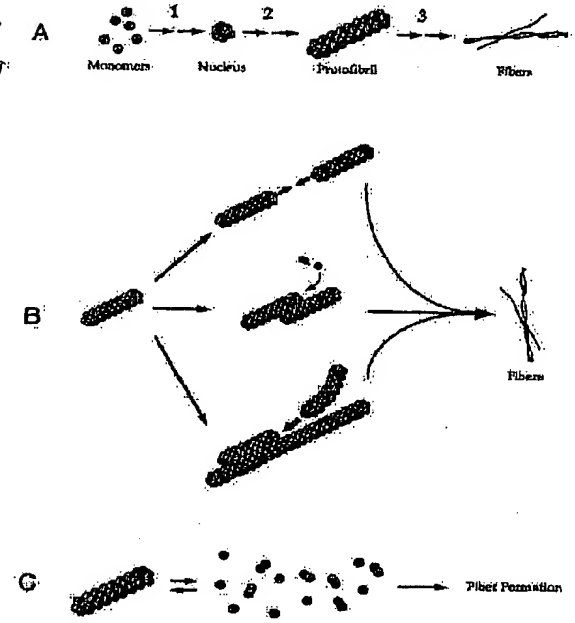

FIG. 7. **Models of Aβ fibrillogenesis.** *A*, Aβ fibrillogenesis is a nucleation-dependent polymerization process in which monomeric Aβ forms nuclei (*step 1*) from which protofibrils emanate (*step 2*). These protofibrils give rise to full-length fibers (*step 3*). *B*, dimers may form nuclei and add to them or to protofibrils, directly. However, dimers may also be in equilibrium with monomers, which might themselves act as the building blocks for these polymeric structures. *C*, besides the addition of Aβ to protofibril ends, protofibrils may give rise to mature fibers through simple end-to-end annealing; lateral association of protofibrils, followed by Aβ addition to ends; and lateral association followed by end-to-end annealing. *D*, it is also possible that protofibrils are incapable of forming fibers directly but instead simply provide precursors for productive pathways of fibrillogenesis. *Note that Aβ and its oligomers and polymers are not drawn to scale.*

obtained by SEC/QLS with those from SDS-PAGE. Fibers, protofibrils, and dimers of Aβ-(1–40) all produced a single ~4-kDa band on gels (Fig. 6*A*). A single band was also seen with dimeric Aβ-(1–42), whereas Aβ-(1–42) protofibrils and fibers produced essentially identical ladders of low molecular weight species ranging from monomer to pentamer (Fig. 6*B*). These results show clearly that SDS-PAGE data do not reliably reflect the polymerization state of Aβ under native conditions. However, the technique may be of use in the characterization of factors that produce detergent-stable multimers.

Modeling Aβ Fibrillogenesis—The structural and kinetic analyses of Aβ fibrillogenesis presented here revealed the existence of a previously unidentified fiber intermediate, the protofibril. The data extant are consistent with a number of models of protofibril formation and conversion into fibers. Each model posits that Aβ monomers combine to form fibril nuclei (Fig. 7*A*, *step 1*), from which protofibrils emanate by linear growth (Fig. 7*A*, *step 2*). These protofibrils, in turn, give rise to the classical 6–10-nm fibers characteristic of neuritic plaques (Fig. 7*A*, *step 3*). During fibrillogenesis, Aβ dimers accumulate initially and then are consumed as protofibrils and fibers form. These dimers may be involved directly in steps 1–3 or may be in equilibrium with monomers, which could be the true building blocks for nuclei, protofibrils, and/or fibers. A dimer "reservoir" could control the monomer concentration and, therefore, the kinetics of fibrillogenesis in the way micelles control fibrillogenesis kinetics at low pH (8, 53).

A number of mechanisms may explain the protofibril→fiber transition (Fig. 7*B*). The simplest is end-to-end association of protofibrils. This is unlikely, however, because of the kinetic barriers associated with the diffusion and proper alignment of protofibril ends. Protofibrils could associate laterally to form "self-templates," onto which precursors (dimers/monomers) could bind and polymerize. Alternatively, lateral association of protofibrils could accelerate end-to-end annealing by fostering proper alignment of protofibril ends. It is also possible that protofibrils are the end-products of a nonfibrillogenic pathway (Fig. 7*C*). In this case, protofibril dissociation would be necessary to release Aβ precursors into productive pathways of fiber formation. Experiments are currently under way to discriminate among these possibilities. Initial results suggest that protofibrils self-associate to produce fibers in the absence of low molecular weight precursors.[8] This mechanism is supported by the failure to observe a continuous distribution of fiber lengths in the size domain between protofibrils and mature amyloid fibers (42).[3]

If protofibrils are key intermediates in Aβ fibrillogenesis *in vivo*, as they appear to be *in vitro*, they would be attractive therapeutic targets because 1) fibrillogenesis mediated through protofibrils might be poisoned with as little as one or two inhibitor molecules per protofibril, and 2) fibrillogenesis inhibitors would function extracellularly. In particular, because the therapeutic levels of inhibitor in the plasma or cerebrospinal fluid would be orders of magnitude lower than those necessary for inhibitors binding to monomeric Aβ, the risk of cytotoxic side-effects would significantly decrease.

Acknowledgments—We thank Dr. John Maggio and William Esler for help with the Aβ RIA, and Marika Ericsson for advice and assistance with electron microscopy. We thank Dr. Peter Lansbury for discussing unpublished data.

REFERENCES

1. Selkoe, D. J. (1991) *Neuron* 6, 487–498
2. Glenner, G. G., and Wong, C. W. (1984) *Biochem. Biophys. Res. Commun.* 120, 885–890
3. Soubert, P., Vigo-Pelfrey, C., Esch, F., Lee, M., Dovey, H., Davis, D., Sinha, S., Schlossmacher, M. G., Whaley, J., Swindlehurst, C., McCormack, R., Wolfert, R., Selkoe, D. J., Lieberburg, I., and Schenk, D. (1992) *Nature* 359, 325–327
4. Busciglio, J., Gabuzda, D. H., Matsudaira, P., and Yankner, B. A. (1993) *Proc. Natl. Acad. Sci. U. S. A.* 90, 2092–2096
5. Selkoe, D. J. (1994) *J. Neuropathol. Exp. Neurol.* 53, 438–447
6. Yankner, B. A. (1996) *Nat. Med.* 2, 850–852
7. Jarrett, J. T., and Lansbury, P. T., Jr. (1993) *Cell* 73, 1055–1058
8. Lomakin, A., Chung, D. S., Benedek, G. B., Kirschner, D. A., and Teplow, D. B. (1996) *Proc. Natl. Acad. Sci. U. S. A.* 93, 1125–1129
9. LeVine, H., III (1993) *Protein Sci.* 2, 404–410
10. Clements, A., Walsh, D. M., Williams, C. H., and Allsop, D. (1993) *Neurosci. Lett.* 161, 17–20
11. Clements, A., Allsop, D., Walsh, D. M., and Williams, C. H. (1996) *J. Neurochem.* 66, 740–747
12. Mantyh, P. W., Ghilardi, J. R., Rogers, S., DeMaster, E., Allen, C. J., Stimson, E. R., and Maggio, J. E. (1993) *J. Neurochem.* 61, 1171–1174
13. Snyder, S. W., Ladror, U. S., Wade, W. S., Wang, G. T., Barrett, L. W., Matayoshi, E. D., Huffaker, H. J., Krafft, G. A., and Holzman, T. F. (1994) *Biophys. J.* 67, 1216–1228
14. Cohen, R. J., and Benedek, G. B. (1975) *Immunochemistry* 12, 349–351
15. Tomaki, S. J., and Murphy, R. M. (1992) *Arch. Biochem. Biophys.* 294, 630–638
16. Shen, C.-L., Scott, G. L., Merchant, F., and Murphy, R. M. (1993) *Biophys. J.* 65, 2383–2395
17. Hilbich, C., Kisters-Woike, B., Reed, J., Masters, C., and Beyreuther, K. (1991) *J. Mol. Biol.* 218, 149–163
18. Burdick, D., Soreghan, B., Kwon, M., Kosmoski, J., Knauer, M., Henschen, A., Yates, J., Cotman, C., and Glabe, C. (1992) *J. Biol. Chem.* 267, 546–554
19. Pike, C. J., Burdick, D., Walencewicz, A. J., Glabe, C. G., and Cotman, C. W. (1993) *J. Neurosci.* 13, 1676–1687
20. Soreghan, B., Kosmoski, J., and Glabe, C. (1994) *J. Biol. Chem.* 269, 28551–28554

[8] D. M. Walsh and D. B. Teplow, unpublished observations.

21. Barrow, C. J., Yasuda, A., Kenny, P. T. M., and Zagorski, M. (1992) *J. Mol. Biol.* **225**, 1075–1093
22. Bush, A. I., Pettingell, W. H., Jr., de Paradis, M., and Tanzi, R. E. (1994) *J. Biol. Chem.* **269**, 12152–12158
23. Kametani, F., Tanaka, K., Tokuda, T., and Allsop, D. (1995) *Brain Res.* **703**, 237–241
24. Nastund, J., Karlstrom, A. R., Tjernberg, L. O., Schierhorn, A., Terenius, L., and Nordstedt, C. (1996) *J. Neurochem.* **67**, 294–301
25. Maggio, J. E., Stimson, E. R., Ghilardi, J. R., Allen, C. J., Dahl, C. E., Whitcomb, D. C., Vigna, S. R., Vinters, H. V., Labenski, M. E., and Mantyh, P. W. (1992) *Proc. Natl. Acad. Sci. U. S. A.* **89**, 5462–5466
26. Esler, W. P., Stimson, E. R., Jennings, J. M., Ghilardi, J. R., Mantyh, P. W., and Maggio, J. E. (1996) *J. Neurochem.* **66**, 723–732
27. Schaggar, H., and Von Jagow, G. (1987) *Anal. Biochem.* **166**, 368–379
28. Pecora, R. (1985) *Dynamic Light Scattering: Applications of Photon Correlation Spectroscopy* (Pecora, R., ed), Plenum Press, New York, NY
29. Kirschner, D. A., Abraham, C., and Selkoe, D. J. (1986) *Proc. Natl. Acad. Sci. U. S. A.* **83**, 503–507
30. Chan, W., Fornwald, J., Brawner, M., and Wetzel, R. (1996) *Biochem.* **35**, 7128–7130
31. Haass, C., Hung, A. Y., Selkoe, D. J., and Teplow, D. B. (1994) *J. Biol. Chem.* **269**, 17741–17748
32. Hendriks, L., Van Duijn, C. M., Cras, P., Cruts, M., Van Hul, W., Van Harskamp, F., Warren, A., McInnis, M. G., Antonarakis, S. E., Martin, J.-J., Hofman, A., and Van Broeckhoven, C. (1992) *Nat. Genet.* **1**, 218–221
33. Levy, E., Carman, M. D., Fernandez-Madrid, I. J., Power, M. D., Lieberburg, I., van Duinen, S. G., Bots, G. T. A. M., Luyendijk, W., and Frangione, B. (1990) *Science* **248**, 1124–1126
34. Podlisny, M. B., Ostaszewski, B. L., Squazzo, S. L., Koo, E. H., Rydell, R. E., Teplow, D. B., and Selkoe, D. J. (1995) *J. Biol. Chem.* **270**, 9564–9570
35. Haass, C. (1996) *Eur. Arch. Psych. Clin. Neurosci.* **246**, 116–123
36. Selkoe, D. J. (1996) *J. Biol. Chem.* **271**, 18295–18298
37. Roher, A. E., Cheney, M. O., Kuo, Y. M., Webster, S. D., Stine, W. B., Haverkamp, L. J., Woods, A. S., Cotter, R. J., Tuohy, J. M., Krafft, G. A., Bonnell, B. S., and Emmerling, M. R. (1996) *J. Biol. Chem.* **271**, 20631–20635
38. Roher, A., Wolfe, D., Palutke, M., and KuKuruga, D. (1986) *Proc. Natl. Acad. Sci. U. S. A.* **83**, 2662–2666
39. Irvine, G. B. (1997) *Anal. Chem. Acta.*, in press
40. Weinreb, P. H., Zhen, W. G., Poon, A. W., Conway, K. A., and Lansbury, P. T., Jr. (1996) *Biochem.* **35**, 13709–13715
41. Perez-Paya, E., Houghten, R. A., and Blondelle, S. E. (1995) *J. Biol. Chem.* **270**, 1048–1056
42. Harper, J. D., Wong, S. S., Lieber, C. M., and Lansbury, P. T., Jr. (1997) *Chem. Biol.* **4**, 119–125
43. Jarrett, J. T., Berger, E. P., and Lansbury, P. T., Jr. (1993) *Biochemistry* **32**, 4693–4697
44. Soto, C., and Castano, E. M. (1996) *Biochem. J.* **314**, 701–707
45. Soto, C., Castano, E. M., Frangione, B., and Inestrosa, N. C. (1995) *J. Biol. Chem.* **270**, 3063–3067
46. Teplow, D. B., Lomakin, A., Benedek, G. B., Kirschner, D. A., and Walsh, D. M. (1997) in *Alzheimer's Disease: Biology, Diagnosis and Therapeutics* (Iqbal, K., Winblad, B., Nishimura, T., Takeda, M., and Wisniewski, H. M., eds) pp. 311–319, John Wiley & Sons Ltd., Chichester, United Kingdom
47. Dill, K. A. (1990) *Biochemistry* **31**, 7133–7155
48. Richardson, J. S., and Richardson, D. C. (1989) in *Prediction of Protein Structures and the Principles of Protein Conformation* (Fasman, G. D., ed) pp. 1–98, Plenum Publishing Corp., New York
49. Minor, D. L., Jr., and Kim, P. S. (1994) *Nature* **367**, 660–663
50. Sisodia, S. S. (1992) *Proc. Natl. Acad. Sci. U. S. A.* **89**, 6075–6079
51. Soto, C., Castano, E. M., Kumar, R. A., Beavis, R. C., and Frangione, B. (1995) *Neurosci. Lett.* **200**, 105–108
52. Fraser, P. E., Mclachlan, D. R., Surewicz, W. K., Mizzen, C. A., Snow, A. D., Nguyen, J. T., and Kirschner, D. A. (1994) *J. Mol. Biol.* **244**, 64–73
53. Lomakin, A., Teplow, D. B., Kirschner, D. A., and Benedek, G. B. (1997) *Proc. Natl. Acad. Sci. U. S. A.* **94**, 7942–7947

L. Brann Patentbyrå AB
Box 1344
751 43 Uppsala

2002-08-22

Ref: US-patentansökan nr. 09/899,915
cc. Prof.Lars Lannfelt

Bästa Ulla,

Refererande till vårt samtal idag, skulle jag vilja att vi går vidare med patentkraven i **grupp VIII** (claim 17-21), method of treatment of Alzheimer's disease. Vidare skulle jag vilja att du besvarar på övriga frågor som kommit upp i US –förläggandet (July 17, 2002) bla.(sequence listing) på sidan 5.
Slutligen skulle jag vilja att du stämmer av nedanstående lista på referenser och patent/patentansökningar med de referenser och patent/patentansökningar som bilades våran ansökan. Skulle vi sakna någon eller några av nedanstående referenser, skulle jag vilja att du kompletterar ansökan med dessa.

Publications:
Walsh D.M. J.Biol. Chem. 272: 22364-22372,1997
Conway etal. Proc. Natl.Acad.Sci. USA 97: 571-576
Kamino K. Etal. Am.L Hum.Genet. 51: 998-1014,1992
Nilsberth etal. Socienty for Neuiroscience Annual Meeting,Miami Beach Nov.1999
Harper J.D. etal. Biochemistry 38:8972-8980, 1999

Patents/patent applications:
EP-B-0 526 511
US 5,753,624
WO 02/03911
WO 01/90182
WO 00/72876
WO 00/72870
WO 00/72880
WO 99/27949
WO 99/27944

Med vänlig hälsning

Pär Gellerfors Docent

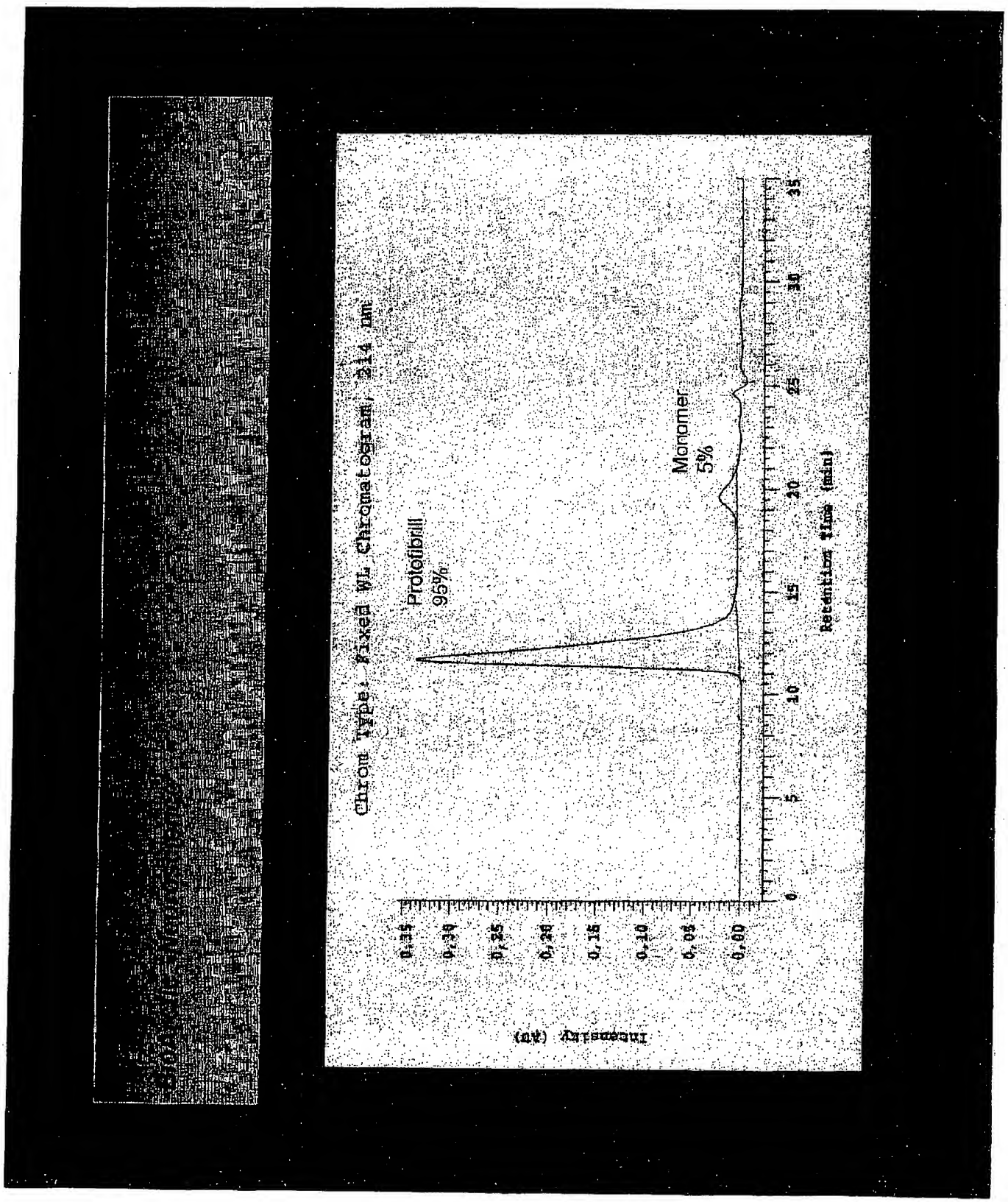
Chrom Type: Fixed WL Chromatogram, 214 nm
Protofibrill
95%
Monomer
5%
Intensity (au)
0.35
0.30
0.25
0.20
0.15
0.10
0.05
0.00
0
5
10
15
20
25
30
35
Retention Time (min)

ELSEVIER

Neuroscience Letters 184 (1995) 90–93

NEUROSCIENCE LETTERS

Amyloid precursor protein mutation at codon 713 (Ala → Val) does not cause schizophrenia: non-pathogenic variant found at codon 705 (silent)

Charlotte Forsell, Lars Lannfelt*

Karolinska Institute, Alzheimer's Disease Research Centre, Department of Clinical Neuroscience, Geriatric Medicine, Huddinge University Hospital, Novum KFC, 141 86 Huddinge, Sweden

Received 31 August 1994; revised version received 18 November 1994; accepted 18 November 1994

Abstract

In some families with early-onset Alzheimer's disease (AD) pathogenic mutations have been found in exons 16 and 17 of the amyloid precursor protein (APP) gene. One case of schizophrenia has been described with a mutation at codon 713. We have developed a single strand conformation polymorphism (SSCP) method that detects mutations in these exons and investigated 98 AD cases and 56 elderly healthy controls. An earlier reported mutation at codon 713 in a healthy control and a previously undescribed polymorphism at codon 705 in a sporadic case of AD were found. These mutations are probably not related to disease pathogenesis.

Keywords: Alzheimer's disease; Schizophrenia; β-Amyloid; Amyloid precursor protein gene; Chromosome 21; Mutation screening; Single strand conformation polymorphism; Chemiluminescence

The neuropathological hallmarks of AD are amyloid plaques and neurofibrillary tangles. The amyloid in the plaques contain a peptide [9] named β-amyloid, which is derived from the amyloid precursor protein (APP) [11,18,29,30]. The APP gene is situated on chromosome 21 and consists of 18 exons, of which parts of exon 16 and 17 encode the β-amyloid fragment [31].

Disease-causing mutations have been found in the APP gene in some early-onset AD families. At codon 717 three different mutations were detected, Val → Ile [6,10,24], Val → Phe [23] and Val → Gly [4] (Table 1). A double-mutation at codon 670/671 (Lys → Asn and Met → Leu) was found in a Swedish AD family [19,22]. A point mutation at codon 693 (Glu → Gln) causes the disorder 'Cerebral haemorrhage with amyloidosis of Dutch type' [20] (Table 1). A mutation at codon 692 (Ala → Gly) has been linked to a slightly different phenotype [13] (Table 1). One case of schizophrenia has been detected with a mutation at codon 713 (Ala → Val) [16] (Table 1). Some other non-pathogenic base substitutions in exons 16 and 17 of the APP gene have been reported [1–3,17,27,28,32] (Table 1).

Mutations in exon 16 and 17 of the APP gene are of great importance in the understanding of the pathogenesis of AD. It is essential to find all mutations at this loci and to investigate their frequency. Single strand conformation polymorphism (SSCP) offers good possibilities for rapid and simple mutation screening. The migration of single-stranded DNA in a non-denaturing polyacrylamide gel is sequence dependent and thus a mutated sequence is detected as a change of mobility caused by its altered structure [26]. Direct DNA sequencing to precisely identify the reason for the changed mobility must, however, be performed.

One affected member from 63 AD families and 35 sporadic AD cases were examined by SSCP. They were all diagnosed according to NINCDS-ADRDA criteria [21]. We also examined 56 elderly healthy controls originating from the Kungsholmen Project [8], who were all without signs of dementia as assessed by mini-mental state examination [7]. DNA was prepared according to standard procedures [14]. In order to investigate the efficiency of the SSCP method, DNA from carriers of the mutations at codons 670/671, 692, 708, 711, 713, 716, the two different mutations at codon 693 and the three at codon 717 were used as positive controls.

* Corresponding author. Tel +46 8 746 55 69; Fax: +46 8 746 52 35.

0304-3940/95/$09.50
SSDI 0304-3940(94)11176-G

Table 1
Mutations in the APP gene, their effects at the protein level, clinical phenotypes and references

Codon	Nucleotide substitution	Amino acid substitution	Phenotype	Cases described	References
Exon 16					
665	G → C	Glu → Asp	–	1 case of AD	[28]
670/671	G → T/A → C	Lys → Asn/Met → Leu	AD	1 Swedish family	[22]
673	G → A	Ala → Thr	–	1 case of stroke and myocardial infarction	[27]
Exon 17					
692	C → G	Ala → Gly	Presenile dementia and cerebral haemorrhage	1 Dutch family	[13]
693	G → C	Glu → Gln	Cerebral haemorrhage	3 Dutch families	[20]
693	A → G	Glu → Gly	–	1 case of AD	[17]
705	C → T	–	–	1 case of AD	[This study]
708	C → T	–	–	3 cases of AD, 1 case of cerebral haemorrhage, 2 non AD, 1 control	[1,2,17]
711	C → A	–	–	1 case of AD	[1]
713	C → T	Ala → Val	–	1 case of schizophrenia, 1 control	[16, this study]
713/715	G → A/G → A	Ala → Thr / –	–	1 case of AD and 5 unaffected family members	[3]
716	C → A	–	–	1 control	[32]
717	G → A	Val → Ile	AD	3 English families, 2 Japanese families	[6,10,24]
717	G → T	Val → Phe	AD	1 American family	[23]
717	T → G	Val → Gly	AD	1 English family	[4]

Amplification of a 216 bp fragment containing exon 16 and a 182 bp fragment containing exon 17 were carried out simultaneously with the 5′ biotinylated primers 1, 2, 3 and 4 (Table 2). SSCP was performed as follows: the PCR product was diluted 1:4 in 1.25% SDS and 12.5 mM EDTA (pH 8.0) and mixed 1:1 in stop solution (USB). After separating the strands at 94°C for 4 min, the samples were cooled on ice and applied to a 5% non-denaturing polyacrylamide gel (30:0.8 acrylamide/bis) using Protogel (National Diagnostics), 10% glycerol and 1× TBE. The gel was electrophoresed at 7 W at room temperature overnight . Thereafter the DNA was capillary transferred to an Immobilon™-S membrane (BioLabs) for 30 min. The DNA strands were visualised using the Polar Plex Chemiluminescent Blotting Kit (BioLabs) and thereafter an X-ray film was exposed to the membrane for 3–5 min.

Table 2
Primer sequences used for PCR amplifications

No.	Exon	Sequence
1	16	5′-GGG TAG GCT TTG TCT TAC AG-3′[a]
2		5′-GGC AAG ACA AAC AGT AGT GG-3′[a]
3	17	5′-GTT TTC AAG GTG TTC TTT GC-3′[a]
4		5′-GGA AAC ATG CAG TCA AGT TTA CC-3′[a]
5		5′-CCT CAT CCA AAT GTC CCC GTC ATT-3′
6		5′-GCC TAA TTC TCT CAT AGT CTT AAT TCC CAC-3′

[a] Indicates biotinylated primers.

To sequence exon 17 a 319 bp fragment was amplified with primers 5 and 6 (Table 2). A second semi-nested PCR reaction using primer 5 and the 5′ biotinylated primer 4 (Table 2) was then performed. Single-stranded DNA was prepared from the second PCR product using streptavidine-coated magnetic beads (Dynabeads) [15] and direct DNA sequencing was performed using Sequenase version 2.0 (USB) according to the manufacturer's instructions. The samples were run on a 6% denaturing polyacrylamide gel, and the sequence was read by eye after exposing an X-ray film to the dried gel.

All positive controls showed extra bands in the SSCP (not shown). Extra bands were also seen close to exon 17 in two of the investigated individuals (Fig. 1). Direct DNA sequencing of exon 17 revealed mutations in both. One was a previously described C → T substitution at codon 713 (Fig. 2A) leading to an amino acid substitution (Ala → Val). This mutation created a restriction site for *Mae*III, and digestion with *Mae*III further confirmed the mutation (not shown). The other was a C → T substitution at codon 705 not previously described (Fig. 2B).

The sensitivity of SSCP is dependent on the length of the amplified fragment, the temperature, the ionic concentrations and the concentration of the gel matrix. Changing these parameters can increase or reduce the separation between fragments of nearly identical sequence. The possibility of detecting mutations in fragments of sizes less than 200 bp is approximately 90%, and for fragments up to 300–350 around 80% [12]. To obtain a short fragment of exon 17 we had to use a primer that covered

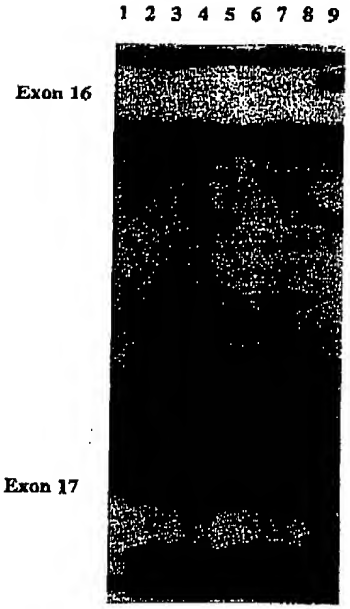

Fig. 1. Detection of sequence variations in exon 16 and 17 by SSCP analysis. A changed pattern was seen in lanes 1, 6 and 9. In lane 1 the 713 mutation is seen, in lane 6 the 705 mutation is demonstrated and lane 9 shows an individual with the 670/671 mutation in exon 16, used as positive control.

eleven nucleotides in the beginning of the exon and mutations at these positions will probably not be detected. However, mutations in this part of exon 17 have not been reported.

In this study, the APP 713 mutation was found in a 76-year-old healthy individual. It has been reported previously in a schizophrenic patient [16], but could not be traced back in the family of the patient and has not been

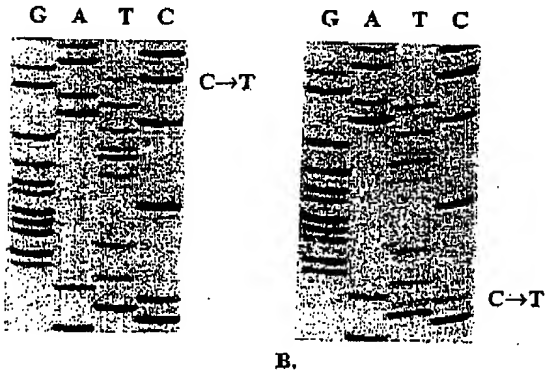

Fig. 2. DNA sequence showing a part of exon 17. (A) A C → T transversion at codon 713, changing Ala → Val, was found in a healthy control. (B) A C → T transversion at codon 705, silent at the protein level, was found in a case of sporadic AD.

seen in investigation of at least 295 patients with schizophrenia [5,25]. Our finding makes it probable that it is unrelated to both schizophrenia and Alzheimer's disease. The mutation at codon 705, first described in this investigation, was silent at the protein level and found in a case of sporadic AD. It was not situated within the acceptor or donor splice junction of the exon, and is probably not involved in mRNA splicing events [31]. This suggests that this variant is unrelated to the pathogenesis of the disease. We conclude that the SSCP method described in this study is well suited to screen for mutations in the APP gene.

Bengt Winblad is thanked for supporting this study. DNA from carriers of different APP mutations were kindly provided by M. Cruts, E. Bakker, M. Abrahamson, S.W. Morris, M.D. Benson, D. Morgan, R. Adroer, G.D. Schellenberg and G.S. Zubenko. The following foundations are acknowledged: Lars Hierta, Torsten och Ragnar Söderberg, Claes Groschinsky, Axelsson-Johnsson, Golje, Martin Rind, Einar Bjelvén, Osterman, Söderström-König, Magnus Bergvall, Gamla Tjänarinnor, the Swedish Municipal Pension Institute, the Bank of Sweden Tercentenary Foundation, King Gustaf V and Queen Victoria's Foundation, the Alzheimer foundation and the Swedish Medical Research Council (project no 10819).

[1] Adroer, R., Lopez-Acedo, C., Oliva, R., Hardy, J. and Fidani, L., A novel silent variant at codon 711 and a variant at codon 708 of the APP sequence detected in Spanish Alzheimer and control cases, Neurosci. Lett., 150 (1993) 33–34.

[2] Balbín, M., Abrahamson, M., Gustafson, L., Nilsson, K., Brun, A. and Grubb, A., A novel mutation in the β-protein coding region of the amyloid β-protein precursor (APP) gene, Hum. Genet., 89 (1992) 580–582.

[3] Carter, D.A., Desmarais, E., Bellis, M., Campion, D., Clerget-Darpoux, F., Brice, A., Agid, Y., Jaillard-Serradt, A. and Mallet, J., More missense in amyloid gene, Nature Genet., 2 (1992) 255–256.

[4] Chartier-Harlin, M.-C., Crawford, F., Houlden, H., Warren, A., Hughes, D., Fidani, L., Goate, A., Rossor, M., Roques, P., Hardy, J. and Mullan, M., Early-onset Alzheimer's disease caused by mutations at codon 717 of the β-amyloid precursor protein gene, Nature, 353 (1991) 844–846.

[5] Coon, H., Hoff, M., Holik, J., Delisi, L.E., Crowe, T., Freedman, R., Shields, G., Boccio, A.M., Lerman, M., Gershon, E.S., Gejman, P.V., Leppert, M. and Byerley, W., C to T nucleotide substitution in codon 713 of amyloid precursor protein gene not found in 86 unrelated schizophrenics from multiplex families, Am. J. Med. Genet., 48 (1993) 36–39.

[6] Fidani, L., Rooke, K., Chartier-Harlin, M.C., Hughes, D., Tanzi, R., Mullan, M., Roques, P., Rossor, M., Hardy, J. and Goate, A., Screening for mutations in the open reading frame and promoter of the β-amyloid precursor protein gene in familial Alzheimer's disease: identification of a further family with APP717 Val → Ile, Hum. Mol. Genet., 13 (1992) 165–168.

[7] Folstein, M.F., Folstein, S.E. and McHugh, P.R., 'Mini-Mental State': a practical method for grading the cognitive state of patients for the clinician, J. Psychiatry Res., 12 (1975) 189–198.

[8] Fratiglioni, L., Grut, M., Forsell, Y., Grafström, M., Holmén, K., Eriksson, K., Viitanen, M., Bäckman, L., Ahlbom, A. and Winblad, B., Prevalence of Alzheimer's disease in an elderly urban

population: relationship with age, sex, and education, Neurology, 41 (1991) 1886–1892.

[9] Glenner, G.G. and Wong, C.W., Alzheimer's disease: initial report of the purification and characterization of a novel cerebrovascular amyloid protein, Biochem. Biophys. Res. Commun., 120 (1984) 885–890.

[10] Goate, A., Chartier-Harlin, M.-C., Mullan, M., Brown, J., Crawford, F., Fidani, L., Giuffra, L., Haynes, A., Irving, N., James, L., Mant, R., Newton, P., Rooke, K., Roques, P., Talbot, C., Pericak-Vance, M., Roses, A., Williamson, R., Rossor, M., Owen, M. and Hardy, J., Segregation of a missense mutation in the amyloid precursor protein gene with familial Alzheimer's disease, Nature, 349 (1991) 704–706.

[11] Goldgaber, D., Lerman, M.I., McBride, O.W., Saffiotti, U. and Gajdusek, D.C., Characterization and chromosomal localization of a cDNA encoding brain amyloid of Alzheimer's disease, Science, 235 (1987) 877–880.

[12] Hayashi, K. and Yandell, D.W., How sensitive is PCR-SSCP?, Hum. Mutation, 2 (1993) 338–346.

[13] Hendriks, L., van Duijn, C.M., Cras, P., Cruts, M., Van Hul, W., van Harskamp, F., Warren, A., McInnis, M.G., Antonarakis, S.E., Martin, J.J., Hofman, A. and Van Broeckhoven, C., Presenile dementia and cerebral haemorrhage linked to a mutation at codon 692 of the β-amyloid precursor protein gene, Nature Genet., 1 (1992) 218–221.

[14] Higuchi, R., Rapid, efficient DNA extraction for PCR from cells or blood, Cetus Corporation, 2 (1989) 1–3.

[15] Hultman, T., Stahl, S., Hornes, E. and Uhlen, M., Direct solid phase sequencing of genomic and plasmid DNA using magnetic beads as solid support, Nucleic Acids Res., 917 (1989) 4937–4946.

[16] Jones, C.T., Morris, S., Yates, C.M., Moffoot, A., Sharpe, C., Brock, D.J.H. and St Clair, D., Mutation in codon 713 of the β-amyloid precursor protein gene presenting with schizophrenia, Nature Genet., 1 (1992) 306–309.

[17] Kamino, K., Orr, H.T., Payami, H., Wijsman, E.M., Alonso, M.E., Pulst, S.M., Anderson, L., O'dahl, S., Nemens, E., White, J.A., Sadovnick, A.D., Ball, M.J., Kaye, J., Warren, A., McInnis, M., Antonarkis, S.E., Korenberg, J.R., Sharama, V., Kukull, W., Larson, E., Heston, L.L., Martin, G.M., Bird, T.D. and Schellenberg, G.D., Linkage and mutational analysis of familial Alzheimer disease kindreds for the APP gene region, Am. J. Hum. Genet., 51 (1992) 998–1014.

[18] Kang, J., Lemaire, H.-G., Unterbeck, A., Salbaum, J.M., Masters, C.L., Grzeschik, K.-H., Multhaup, G., Beyreuther, K. and Müller-Hill, B., The precursor of Alzheimer's disease amyloid A4 protein resembles a cell-surface receptor, Nature, 325 (1987) 733–736.

[19] Lannfelt, L., Bogdanovic, N., Appelgren, H., Axelman, K., Lilius, L., Hansson, O., Schenk, D., Hardy, J. and Winblad, B., Amyloid precursor protein mutation causes Alzheimer's disease in a Swedish family, Neurosci. Lett., 168 (1994) 254–256.

[20] Levy, E., Carman, M.D., Fernandez-Madrid, I.J., Power, M.D., Lieberburg, I., van Duinen, S.G., Bots, G.T.A.M., Luyendijk, W. and Frangione, B., Mutation of the Alzheimer's disease amyloid gene in hereditary cerebral haemorrhage, Dutch type, Science, 248 (1990) 1124–1126.

[21] McKhann, G., Drachman, D., Folstein, M. Katzman, R., Price, D. and Stadlan, E.M., Clinical diagnosis of Alzheimer's disease: report of the NINCDS-ARDRA work group under the auspices of Department of Health and Human Services task force on Alzheimer's disease, Neurology, 34 (1984) 939–944.

[22] Mullan, M., Crawford, F., Axelman, K., Houlden, H., Lilius, L., Winblad, B. and Lannfelt, L., A pathogenic mutation for probable Alzheimer's disease in the APP gene at the N-terminus of β-amyloid, Nature Genet., 1 (1992) 345–347.

[23] Murrell, J., Farlow, M., Ghetti, B. and Benson, M.D., A mutation in the amyloid precursor protein associated with hereditary Alzheimer's disease, Science, 254 (1991) 97–99.

[24] Naruse, S., Igarashi, S., Kobayashi, H., Aoki, K., Inuzuka, T., Kaneko, K., Shimizu, T., Iihara, K., Kojima, T., Miyatake, T. and Tsuji, S., Mis-sense mutation Val → Ile in exon 17 of amyloid precursor protein gene in Japanese familial Alzheimer's disease, Lancet, 337 (1991) 978–979.

[25] Nöthen, M.M., Erdmann, J., Propping, P., Lanczik, M., Rietschel, M., Körner, J., Maier, W., Albus, M., Ertl, M.A. and Wildenauer, D.B., Mutation in the β amyloid precursor protein gene and schizophrenia, Biol. Psychiatry, 34 (1993) 502–504.

[26] Orita, M., Suzuki, Y., Sekiya, T. and Hayashi, K., A rapid and sensitive detection of point mutations and genetic polymorphisms using polymerase chain reaction, Genomics, 5 (1989) 874–879.

[27] Peacock, M.L., Warren, J.T., Roses, A.D. and Fink, J.K., Novel polymorphism in the A4 region of the amyloid precursor protein gene in a patient without Alzheimer's disease, Neurology, 43 (1993) 1254–1256.

[28] Peacock, M.L., Murman, D.L., Sima, A.A.F., Warren, J.T., Roses, A.D. and Fink, J.K., Novel amyloid precursor protein gene mutation (codon 665^{Asp}) in a patient with late-onset Alzheimer's disease, Ann. Neurol., 35 (1994) 432–438.

[29] Robakis, N.K., Ramakrishna, N., Wolfe, G. and Wisniewski, H.M., Molecular cloning and characterization of a cDNA encoding the cerebrovascular and the neuritic plaque amyloid peptides, Proc. Natl. Acad. Sci. USA, 84 (1987) 4190–4194.

[30] Tanzi, R.E., Gusella, J.F., Watkins, P.C., Bruns, G.A.P., St George-Hyslop, P., Van Keuren, M.L., Patterson, D., Pagan, S., Kurnit, D.M. and Neve, R.L., Amyloid β protein gene: cDNA, mRNA distribution, and genetic linkage near the Alzheimer locus, Science, 235 (1987) 880–884.

[31] Yoshikai, S.-i., Sasaki, H., Doh-ura, K., Furuya, H. and Sakaki, Y., Genomic organization of the human amyloid beta-protein precursor gene, Gene, 87 (1990) 257–263.

[32] Zubenko, G.S., Farr, J., Stiffler, J.S., Hughes, H.B. and Kaplan, B.B., Clinically-silent mutation in the putative iron-responsive element in exon 17 of the β-amyloid precursor protein gene, J. Neuropathol. Exp. Neurol., 51 (1992) 459–463.